Grasp Compliance Regulation in Synergistically Controlled Robotic Hands with VSA

Edoardo Farnioli[1,2], Marco Gabiccini[1,2,3], Manuel Bonilla[1], Antonio Bicchi[1,2]

Abstract— **In this paper, we propose a general method to achieve a desired grasp compliance acting both on the joint stiffness values and on the hand configuration, also in the presence of restrictions caused by synergistic underactuation. The approach is based on the iterative exploration of the equilibrium manifold of the system and the quasi-static analysis of the governing equations. As a result, the method can cope with large commanded variations of the grasp stiffness with respect to an initial configuration. Two numerical examples are illustrated. In the first one, a simple 2D hand is analyzed so that the obtained results can be easily verified and discussed. In the second one, to show the method at work in a more realistic scenario, we model grasp compliance regulation for a DLR/HIT hand II grasping a ball.**

I. INTRODUCTION

The human hand is an extraordinary example of dexterity and complexity. To imitate human dexterity, the developments of robotic hands was directed, over the years, to increase the number of degrees of freedom (DoFs), arriving to admirable example of technological design [1], [2], [3]. However, complex kinematic structures bring difficulties in control and, for this sake, some underactuation mechanisms were studied [4], [5]. Recent works get inspiration from humans to properly design effective underactuation systems. A large data set of human grasp postures was analysed via PCA, finding the presence of preferential joint movement patterns, also called *synergies*. This concept was implemented in robotic devices as a correlation between hand joints during the movements, both via hardware and software control [6], [7]. The possibility to adapt the hand was introduced with an elastic approach [8], called *soft synergy*, where the synergistic movement is imposed to a reference hand. Despite the fact that the soft synergies approach are not easy to implement in an hardware device, in [9] the authors demonstrated the possibility to obtain the similar effects using tendon driven systems, called *adaptive synergy*. The result is a hand able to adapt its shape and to achieve a stable grasp of a huge set of common objects.

This work is supported by the EC under the CP-IP grant no. 248587 "THE Hand Embodied", within the FP7-2007-2013 program "Cognitive Systems and Robotics", ERC Advanced Grant no. 291166 "SoftHands" - A Theory of Soft Synergies for a New Generation of Artificial Hands- and FP7/2007-2013 grant agreement no. 257462 "HYCON2 Network of excellence', and by the grant no. 600918 "PaCMan", within the FP7-ICT-2011-9 program "Cognitive Systems".

[1]Research Center "E. Piaggio", Università di Pisa, Largo Lucio Lazzarino 1, 56122 Pisa, Italy

[2]Department of Advanced Robotics, Istituto Italiano di Tecnologia, Via Morego 30, 16163 Genova, Italy

[3]Department of Civil and Industrial Engineering, Università di Pisa, Largo Lucio Lazzarino 1, 56122 Pisa, Italy

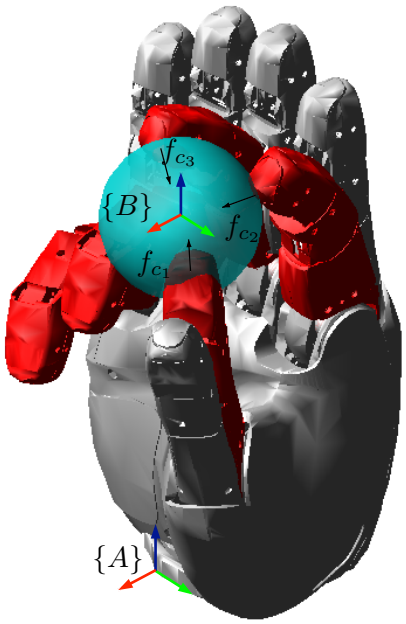

Fig. 1: DLR/HIT Hand II endowed with joint impedance control, underactuated via software according to the soft-synergy paradigm [**8**].

An other important feature studied during the last few years, is the possibility to control the joint stiffness values. This aspect is crucial, for example, when accidental collisions can occur both with the humans and with the environment. The first strategy to cope with these events is based on the application of proper control strategies, to establish a desired joint displacement in consequence of a certain load [10]. The second one is obtained by elastic actuators that can change their stiffness [11], [12].

Both the contribution of variable stiffness joints and underactuation are important in the problem of the grasp compliance regulation: the first one affecting the grasp compliance matrix, the second one reducing the space of reachable hand/object configurations.

In this paper, a mathematical model of grasping in presence of both variable stiffness joints and synergistic underactuation is considered with the aim to evaluate and control grasp compliance. Key to this objective, is the introduction in Sec. II of the *grasp compliance* matrix. The proposed approach is based on two main concepts: the *equilibrium manifold of the grasp*, discussed in section III, and its *tangent space*, discussed in section IV. While the first one defines equilibrium configurations of the system, the second one is instrumental to the computation of local grasp compliance. In section V we present an optimization method, based on a trust-region approach, able to steer the system towards a desired grasp compliance while moving over the equilibrium

manifold.

Numerical examples, section VI, show the effectiveness of proposed method by considering (i) a simple planar gripper and (ii) the DLR/HIT hand grasping a ball. Both cases are studied considering the possibility to change (i) the joint stiffness, (ii) the synergistic references or (iii) both.

II. Problem Statement

With the term *grasp compliance*, we refer to the map between the generalized forces acting on the grasped object and its consequent displacement. In particular, we consider a virtual kinematic chain connecting an inertial frame and a frame attached to the object. The grasp compliance that we consider in this paper is the map between the joint torques and the joint displacements of this virtual kinematic chain.

Many are the parameters that influence the grasp compliance matrix: the number and the nature of the contact points, the presence of compliant joints, and others. From an analytical point of view, the grasp compliance is a matrix $C_g \in \mathbb{R}^{6\times 6}$ such that

$$\delta u = C_g \delta w, \tag{1}$$

where $\delta u, \delta w \in \mathbb{R}^6$ are the generalized displacements and forces acting on the object, respectively. Denoting with $\varphi \in \mathbb{R}^{\sharp\varphi}$ a vector collecting all the forces and the configuration variables describing a grasping problem, where $\sharp\varphi$ indicates the dimension of the vector φ, we can write the grasp compliance matrix as a function of the form

$$C_g = C_g(\varphi) : \mathbb{R}^{\sharp\varphi} \to \mathbb{R}^{6\times 6}. \tag{2}$$

Despite the fact that a definition of the compliance is possible also for dynamic problems, we just focus on static equilibrium configurations. With this in mind, the admissible configurations are those $\bar{\varphi} : E(\bar{\varphi}) = 0$, where $E(\bullet)$ is the *equilibrium constraint* of the whole system, that has null value if and only if the system is in equilibrium. In other words, we focus on compliance matrices computed as

$$C_g = C_g(\bar{\varphi}) : \mathbb{E} \subseteq \mathbb{R}^{\sharp\varphi} \to \mathbb{C}_g \subseteq \mathbb{R}^{6\times 6}, \tag{3}$$

where $\mathbb{E}$ and $\mathbb{C}_g$ are suitable subspaces. In this paper, we suggest a method to explore the space $\mathbb{E}$ with the aim to find an equilibrium configuration where the grasp compliance is the closest possible to a given one.

III. Equilibrium Manifold of the Grasp

The global equilibrium constraint can be imposed by studying the elemental parts composing the system. The notation adopted is summarized in Table I. The underlying analytical framework is based on [13], [14].

Notation	Definition
δx	variation of variable x
$\bar{x}$	value of x in the equilibrium configuration
$\sharp x$	dimensions of vector x
$q \in \mathbb{R}^{\sharp q}$	joint parameters
$q_r \in \mathbb{R}^{\sharp q}$	reference joint parameters
$k_q \in \mathbb{R}^{\sharp q}$	joint stiffness
$\tau \in \mathbb{R}^{\sharp q}$	joint torques
$\sigma \in \mathbb{R}^{\sharp\sigma}$	synergistic parameters
$\eta \in \mathbb{R}^{\sharp\sigma}$	synergistic generalized forces
n	number of contact points
c	number of contact constraints acting on the object
$u \in \mathbb{R}^6$	joint parameters of the virtual kinematic chain, parametrize the object configuration
$p^c_{ab} \in \mathbb{R}^c$	pose of frame $\{B\}$ with respect to $\{A\}$ in components $\{C\}$
$\xi^c_{ab} \in \mathbb{R}^6$	twist of frame $\{B\}$ with respect to $\{A\}$ in components $\{C\}$
$v^c_{ab} \in \mathbb{R}^c$	contact point velocity in the constrained directions
$t^b_a \in \mathbb{R}^{\sharp t}$	compact form for t^b_{ab}, if t is a velocity or a twist
$f^o_h \in \mathbb{R}^c$	contact force/torque vector exerted by the hand on the object
$w^b_e \in \mathbb{R}^6$	external wrench on the object
$w \in \mathbb{R}^6$	joint torques of the virtual kinematic chain, parametrize the external wrench on the object
${}^bJ_v \in \mathbb{R}^{6\times 6}$	body Jacobian of the virtual kinematic chain
${}^oJ \in \mathbb{R}^{c\times \sharp q}$	hand Jacobian matrix in contact frame
$S \in \mathbb{R}^{\sharp q\times\sharp\sigma}$	synergy matrices
${}^bG \in \mathbb{R}^{6\times c}$	grasp matrix in body frame
$\Phi^\star$	*Fundamental Grasp Matrix*, the coefficient matrix of the *Fundamental Grasp Equation* (29)
φ	*augmented configuration*, vector collecting all the variables of the system

TABLE I: Notation used for grasp analysis.

A. Equilibrium of the Object

The interaction between the hand and the grasped object usually occurs at many points. On the i^{th} contact point on the object, we consider a frame of reference $\{O_i\}$. In this frame we describe the i^{th} interaction force $f^{o_i}_{h_i} \in \mathbb{R}^{c_i}$, exerted by the hand contact frame $\{H_i\}$ on the object. The dimension c_i depends on the nature of the local contact [13]. Introducing a frame of reference $\{B\}$ attached to the object to mark its posture with respect to an inertial frame $\{A\}$, we indicate with $w^b_e \in \mathbb{R}^6$ an external wrench acting on the object, with components in $\{B\}$. Using this definitions, the equilibrium equation for the object can be expressed as

$$w^b_e + {}^bG f^o_h = 0, \tag{4}$$

where ${}^bG \in \mathbb{R}^{6\times c}$ is the *grasp matrix in body frame* [14], $c = \sum_{i=1}^{p} c_i$ is the total number of contact constraints, and $f^o_h \in \mathbb{R}^c$ is a vector collecting all the hand/object interaction forces.

An alternative description of the external wrench can be obtained using generalized forces after a suitable parametrization for the object configuration has been introduced. To this aim, we consider a virtual kinematic chain linking together the inertial frame $\{A\}$ and the object frame $\{B\}$. An intuitive choice is to consider three prismatic joints, aligned with X, Y and Z respectively, followed by three rotational joints, with the same disposition. It is now easy to describe the twist of the object frame by virtue of the body Jacobian [13] of the virtual kinematic chain ${}^bJ_v(u) \in \mathbb{R}^{6\times 6}$, thus obtaining

$$\xi^b_a = {}^bJ_v(u)\dot{u}. \tag{5}$$

By kineto-static duality, defining the vector $w \in \mathbb{R}^6$ as the vector collecting the joint forces/torques of the virtual chain, it can be written that

$$w = {}^bJ_v(u)^T w^b_e. \tag{6}$$

From (6) it follows that the virtual chain can be employed to parameterize the external wrench in body frame. Combining (6) and (4), we get

$$w = {}^bJ_v(u)^T {}^bG f^o_h := {}^vG(u) f^o_h, \tag{7}$$

that describes the equilibrium of the object in terms of contact forces and joint torques of the virtual kinematic chain.

B. Equilibrium of the Hand

On the i^{th} contact point we consider the frame $\{H_i\}$ attached to the hand. We can describe its twist using the spatial Jacobian matrix, according to the law

$$\xi^a_{ah_i} = {}^aJ_i(q_i)\dot{q}_i, \tag{8}$$

where $q_i \in \mathbb{R}^{\sharp q_i}$ is the vector collecting the joint variables that affects the motion of $\{H_i\}$. According to (7), where we used contact forces expressed in a local frame attached to the object, similarly we need to express the twist in (8) in the frame $\{O_i\}$. To this aim, we make use of the *adjoint operator*, that acts on twists and wrenches as described in [13]. Thus, defining ${}^{o_i}J_i(q_i,u) = \text{Ad}_{g_{o_ia}(u)}{}^aJ_i(q_i)$, it immediately follows that

$$\xi^{o_i}_{ah_i} = {}^{o_i}J_i(q_i,u)\dot{q}_i. \tag{9}$$

Since the hand is in contact with the object, some components of the contact frame velocity move along directions forbidden by the contact interaction. These components can be extracted from the complete twist in (9) by the use of a proper *selection matrix* $B_i^T \in \mathbb{R}^{c_i\times 6}$ as

$$v^{o_i}_{ah_i} = B_i^T\xi^{o_i}_{ah_i}. \tag{10}$$

As discussed in [13], the particular expression of the selection matrix in (10) depends on the nature of the contact.

Considering the whole system, we define $v^o_{ah} \in \mathbb{R}^c$ as the vector containing all contact velocities, and $q \in \mathbb{R}^{\sharp q}$ as the vector containing all the joint variables. From these, properly combining the expression for each contact points in (10), we can finally write

$$v^o_{ah} = {}^oJ(q,u)\dot{q}, \tag{11}$$

where ${}^oJ(q,u) \in \mathbb{R}^{c\times\sharp q}$ is the hand Jacobian matrix.

From eq. (11), again by duality arguments, we write the equilibrium equation for the hand, resulting in

$$\tau = {}^oJ(q,u)^T f^o_h, \tag{12}$$

where $\tau \in \mathbb{R}^{\sharp q}$ is the vector of the joint torques of the hand.

C. Equilibrium of the Contact Virtual Springs

As in multifingered grasping the contact force distribution problem is statically indeterminate, we introduce a penalty formulation of the contact. To proper describe this model, for the i^{th} contact point, we consider a virtual spring, whose extremities are attached to the hand contact frame $\{H_i\}$, and to the object contact frame $\{O_i\}$. Without loss of generality we assume that the configuration of the two contact frames is such that they are parallel when no contact force exists. Thus, indicating with $\tilde{p}^{o_i}_{o_ih_i} \in \mathbb{R}^6$ a vector describing the configuration of $\{H_i\}$ with respect to $\{O_i\}$, with components in $\{O_i\}$, the contact interaction force can be expressed as

$$f^{o_i}_{h_i} = K_{c_i}B_i^T\tilde{p}^{o_i}_{o_ih_i} := K_{c_i}p^{o_i}_{o_ih_i}, \tag{13}$$

where $K_{c_i} \in \mathbb{R}^{c_i\times c_i}$ is the stiffness matrix[1] for the i^{th} contact. In eq. (13) we defined $p^{o_i}_{o_ih_i} = B_i^T\tilde{p}^{o_i}_{o_ih_i} \in \mathbb{R}^{c_i}$, that is the *selected configuration vector*, containing only the terms of the mutual configuration of the contact frames able to strain the virtual spring.

Considering all the contacts, introducing the contact stiffness matrix $K_c \in \mathbb{R}^{c\times c}$, the equilibrium law for the virtual contact springs can be globally expressed as

$$f^o_h = K_c\, p^o_{oh}. \tag{14}$$

D. Equilibrium of the Elastic Joints

The elasticity of the i^{th} joint can be properly described considering a spring with stiffness $k_{q_i} \in \mathbb{R}$, acting between the actual value of the joint variable, and the value of a joint reference variable $q_{r_i} \in \mathbb{R}$. Globally, the equilibrium of the elastic joint actuation can be written as $\tau = K_q(q_r - q)$, where $q_r \in \mathbb{R}^{\sharp q}$ is a vector collecting all the joint references, and $K_q \in \mathbb{R}^{\sharp q\times\sharp q}$ is the joint stiffness matrix, such that $K_{q_{ij}} \in \{k_{q_i}, 0\}$, where the latter is chosen for $i \neq j$.

E. Equilibrium of the Synergistic Underactuation

A synergistic underactuation is a correlation between reference joint angles, that is

$$q_r = S\sigma, \tag{15}$$

where $S \in \mathbb{R}^{\sharp q\times\sharp\sigma}$, with $\sharp\sigma \leq \sharp q$, is the *synergy matrix*[2].

Introducing the vector $\eta \in \mathbb{R}^{\sharp\sigma}$ describing the generalized actuation forces at the synergy level, by kineto-static duality, from (15) it follows

$$\eta = S^T\tau, \tag{16}$$

that describes the equilibrium condition for the underactuation.

F. The Equilibrium Manifold

The equilibrium of the whole system is achieved if the conditions (7), (12), (14), (15) and (16) are together verified. The consequent system of equations can be written as

$$\begin{cases} w + {}^vG(u)f^o_h &= 0 \\ \tau - {}^oJ^T(q,u)f^o_h &= 0 \\ f^o_h - K_c\, p^o_{oh} &= 0 \\ \tau - K_q(S\sigma - q) &= 0 \\ \eta - S^T\tau &= 0, \end{cases} \tag{17}$$

which is an algebraic nonlinear system of the form $E(\varphi)$=0, where $\varphi = \left[u^T, f^{oT}_h, \tau^T, q^T, \eta^T, w^T, k^T_q, \sigma^T\right]^T \in \mathbb{R}^{\sharp\varphi}$ is the *augmented configuration* of the system. In other words, as follows from the definitions in previous sections, a configuration of the system $\bar{\varphi}$ is such that $E(\bar{\varphi}) = 0$ if and only if it is an equilibrium.

[1]Note that the configuration vector needs a parametrization for its rotational part. This choice has influence on the expression of the contact stiffness matrix.

[2]We consider here to use a constant synergy matrix, as the one resulting from [15]. However, the treatment can be easily extended to the case in which the synergy matrix is a function of the configuration of the system.

IV. Tangent Space of the Equilibrium Manifold

As pointed out in (1), the grasp compliance matrix relates small variations of external forces and object displacements. In this section, we will show how to compute the grasp compliance matrix studying the tangent space of the equilibrium manifold in (17). For later use, we remind that, for a generic function $F(\alpha, \beta)$, and for $\bar{\alpha}, \bar{\beta} : F(\bar{\alpha}, \bar{\beta}) = 0$, a small variation of the variables implies a first order variation of the function in the form

$$F(\bar{\alpha} + \delta\alpha, \bar{\beta} + \delta\beta) \simeq F_{,\alpha}(\bar{\alpha}, \bar{\beta})\delta\alpha + F_{,\beta}(\bar{\alpha}, \bar{\beta})\delta\beta \quad (18)$$

A. Perturbation of the Object Equilibrium

Applying (18) to (7), we obtain a description of the perturbation of the equilibrium law for the object as

$$\delta w + {}^v\bar{G}\delta f_h^o + \bar{U}_g \delta u = 0, \quad (19)$$

where we introduced matrix $\bar{U}_g := \left[\partial_u {}^vG(u)\bar{f}_h^o\right]_{\bar{\varphi}} \in \mathbb{R}^{6\times 6}$.

B. Perturbation of the Hand Equilibrium

Similarly to what previously done, applying (18) to (12), we arrive at

$$\delta\tau - \bar{Q}_j\delta q - \bar{U}_j\delta u - {}^o\bar{J}^T\delta f_h^o = 0, \quad (20)$$

where we introduced the following matrices $\bar{Q}_j = \left[\partial_q {}^oJ^T(q,\bar{u})\bar{f}_h^o\right]_{\bar{\varphi}} \in \mathbb{R}^{\sharp q\times\sharp q}$ and $\bar{U}_j = \left[\partial_u {}^oJ^T(\bar{q},u)\bar{f}_h^o\right]_{\bar{\varphi}} \in \mathbb{R}^{\sharp q\times 6}$.

C. Perturbation of the Contact Springs

As described in section III-C, the contact model is obtained by considering a virtual spring whose ends are attached to the hand and to the object, respectively. In order to describe the perturbation of the contact forces around an equilibrium configuration, we look for an analytical description of the contact frame displacements. Considering the hand Jacobian, we can easily observe that, from the equation describing the contact frame velocity

$$v_h^o = {}^oJ(q,u)\dot{q}, \quad (21)$$

multiplying each member for dt, we obtain

$$\delta C_{ah}^o = {}^oJ(q,u)\delta q, \quad (22)$$

where $\delta C_{ah}^o \in \mathbb{R}^c$ is a vector collecting the displacements of the hand contact frames. Considering (4), by kineto-static considerations, it immediately follows that the transpose of the grasp matrix is the map from the object frame twist $\xi_a^b \in \mathbb{R}^6$, and the contact frame velocities $v_{ab}^o \in \mathbb{R}^c$, obtaining

$$v_{ab}^o = {}^bG^T\xi_a^b. \quad (23)$$

However, for a description of the object twists ξ_a^b in terms of variation of true coordinates it is necessary to introduce a parametrization of $SE(3)$. This can be made considering again the virtual kinematic chain linking together the inertial frame $\{A\}$ and the object frame $\{B\}$. In fact, substituting (5) in (23) and multiplying each member for dt, we obtain

$$\delta C_a^o = {}^bG^T{}^bJ_v(u)\delta u = {}^vG^T(u)\delta u. \quad (24)$$

Thus, considering (22) and (24), we can write the differential form of (14) as

$$\delta f_h^o = K_c\left({}^o\bar{J}\delta q - {}^v\bar{G}^T\delta u\right). \quad (25)$$

D. Perturbation of the Elastic Joints

Taking into account the possibility to control the joint stiffness, evaluating the differential of the joint constitutive equations, we obtain

$$\delta\tau = \bar{K}_q\left(\delta q_r - \delta q\right) + \left[\partial_{k_q}K_q(\bar{q}_r - \bar{q})\right]_{\bar{\varphi}}\delta k_q. \quad (26)$$

Remembering that, by definition, $K_q = \mathrm{diag}(k_q)$, it easily follows that

$$\left[\partial_{k_q}K_q(\bar{q}_r - \bar{q})\right]_{\bar{\varphi}} = \mathrm{diag}\left(\bar{q}_r - \bar{q}\right). \quad (27)$$

Thus, defining the matrix $\bar{D}_{k_q} = \mathrm{diag}\left(\bar{q}_r - \bar{q}\right) \in \mathbb{R}^{\sharp q\times\sharp q}$, from (27) and (26), the first order perturbation of the equilibrium of the hand can be written as

$$\delta\tau = \bar{K}_q\left(\delta q_r - \delta q\right) + \bar{D}_{k_q}\delta k_q. \quad (28)$$

E. Perturbation of the Synergistic Underactuation

The joint and the synergistic configuration variables are related by (15). By differentiation we obtain that the configuration perturbations can be written as

$$\delta q_r = S\delta\sigma. \quad (30)$$

Similarly, the joint torque and the synergistic force variations are related by the differential of (16), that is

$$\delta\eta = S^T\delta\tau. \quad (31)$$

F. The Fundamental Grasp Equation and the Grasp Compliance Matrix

Considering together equations (19), (20), (25), (28), (30) and (31), we obtain a constraint for the first order perturbation of the grasp variables, with respect to an equilibrium configuration. The result, called *fundamental grasp equation* (FGE), is a *linear* and *homogeneous*, system of equations (29). From the previous considerations it follows that any variation of the augmented configuration, with respect to the equilibrium point, $\delta\varphi \in \mathbb{R}^{\sharp\varphi}$, satisfying (29) lies on the tangent space of the equilibrium manifold, evaluated at the equilibrium configuration $\bar{\varphi}$. Eq. (29) can be written in compact form as $\Phi^\star\delta\varphi = 0$, where $\Phi^\star \in \mathbb{R}^{r_\Phi\times c_\Phi}$, with $c_\Phi = \sharp\varphi$, is called *fundamental grasp matrix* (FGM).

From the properties of the system (29) it follows that a basis of its solution space is described by a basis for the nullspace of the FGM, that is by a matrix $\Gamma \in \mathbb{R}^{r_\Gamma\times c_\Gamma}$, with $r_\Gamma = c_\Phi$, such that $\Phi^\star\Gamma = 0$. From direct inspection of (29), the following relationships hold $r_\Phi = \sharp w + \sharp f + 2\sharp q + \sharp\sigma$, and $c_\Phi = 2\sharp w + \sharp f + 3\sharp q + 2\sharp\sigma$. This implies that, if the FGM is full row-rank, as it happens for the most common configuration of practical interest, its nullspace has dimension $c_\Gamma = c_\Phi - r_\Phi = \sharp w + \sharp q + \sharp\sigma$. As a consequence, a perturbation of the system is completely described when a number of variables equal to c_Γ is given. In this case, we consider to know the external wrench, the joint stiffness and the synergy variation, and we will refer to them as the *independent variables* of the system, $\delta\varphi_i = \left[\delta w^T, \delta k_q^T, \delta\sigma^T\right]^T \in \mathbb{R}^{\sharp\varphi_i}$, where $\sharp\varphi_i = c_\Gamma$. Conversely, the vector of *dependent variables* is defined as $\delta\varphi_d = \left[\delta u^T, \delta f_h^{oT}, \delta\tau^T, \delta q^T, \delta\eta^T\right]^T \in \mathbb{R}^{\sharp\varphi_d}$, where $\sharp\varphi_d = r_\Phi$. Therefore, eq. (29) can be written as

$$\Phi^\star\delta\varphi = \begin{bmatrix}\Phi_d^\star & \Phi_i^\star\end{bmatrix}\begin{bmatrix}\delta\varphi_d \\ \delta\varphi_i\end{bmatrix} = 0, \quad (32)$$

$$\begin{bmatrix} \bar{U}_g & {}^v\bar{G} & 0 & 0 & 0 & I_{\sharp w} & 0 & 0 \\ -\bar{U}_j & {}^o\bar{J}^T & I_{\sharp\tau} & -\bar{Q}_j & 0 & 0 & 0 & 0 \\ K_c{}^v\bar{G}^T & I_{\sharp f} & 0 & -K_c{}^o\bar{J} & 0 & 0 & 0 & 0 \\ 0 & 0 & I_{\sharp\tau} & \bar{K}_q & 0 & 0 & \bar{D}_{K_q} & -\bar{K}_q S \\ 0 & 0 & -S^T & 0 & I_{\sharp\sigma} & 0 & 0 & 0 \end{bmatrix} \begin{bmatrix} \delta u \\ \delta f_h^o \\ \delta\tau \\ \delta q \\ \delta\eta \\ \delta w \\ \delta k_q \\ \delta\sigma \end{bmatrix} = 0 \tag{29}$$

where, by construction, $\Phi_d^\star \in \mathbb{R}^{r_\phi \times r_\phi}$ and $\Phi_i^\star \in \mathbb{R}^{r_\phi \times c_\Gamma}$. From linear algebra it is known that $\mathcal{N}(A) = \mathcal{N}(MA)$, if M is a full-rank square matrix [16]. This implies that we can pre-multiply (32) by a suitable matrix without affecting its solution space. In particular, choosing $M = \Phi_d^{\star -1}$ we obtain

$$\Phi\delta\varphi = \begin{bmatrix} I_{r_\phi} & \Phi_i \end{bmatrix} \begin{bmatrix} \delta\varphi_d \\ \delta\varphi_i \end{bmatrix} = 0, \tag{33}$$

where $\Phi_i = \Phi_d^{\star -1}\Phi_i^\star \in \mathbb{R}^{r_\phi \times c_\Gamma}$. The new coefficient matrix Φ is said the *canonical form of the fundamental grasp matrix* (cFGM). From (33) it immediately follows that

$$\delta\varphi_d = -\Phi_i\delta\varphi_i. \tag{34}$$

More explicitly, a variation of a generic dependent variable $\delta x_d \in \left\{\delta u^T, \delta f_h^{oT}, \delta\tau^T, \delta q^T, \delta\eta^T\right\}$ can be written in the form

$$\delta x_d = \Omega_{x_d}\delta w + X_{x_d}\delta k_q + \Psi_{x_d}\delta\sigma, \tag{35}$$

where $\Omega_{x_d} \in \mathbb{R}^{\sharp x_d \times 6}$, $X_{x_d} \in \mathbb{R}^{\sharp x_d \times \sharp q}$ and $\Psi_{x_d} \in \mathbb{R}^{\sharp x_d \times \sharp\sigma}$ are the blocks composing $-\Phi_i$ in (34).

From (35), the explicit relationship for the object displacement variable appears as

$$\delta u = \Omega_u\delta w + X_u\delta k_q + \Psi_u\delta\sigma. \tag{36}$$

By inspection of (36), it is evident that matrix Ω_u is the map between the external forces on the object and the consequent object displacement, when no actuation is commanded to the hand. Therefore, the grasp compliance matrix is $C_g = \Omega_u$. It is important to note that the grasp compliance was obtained using the block elements composing the FGM. As a consequence, we will obtain $C_g = C_g(\varphi)$. From direct inspection of the FGM, stricter conditions can be found about the dependence of the compliance matrix upon the variables of the system. However, this discussion is avoided here for space limitations.

V. Grasp Compliance Regulation Algorithm

Given a configuration of the system $\hat{\varphi}$, we define the *equilibrium residual vector* as $r_e = E(\hat{\varphi}) \in \mathbb{R}^{r_\Phi}$. Considering the independent variables of the system as fixed, it is possible to find the dependent ones such that the configuration is an equilibrium point. This problem can be framed as a nonlinear least-squares one and its solution found by minimizing the quadratic misfit $l(\varphi_d) = \frac{1}{2}r_e^T(\varphi_d)W_e r_e(\varphi_d)$, where $W_e \in \mathbb{R}^{r_\Phi \times r_\Phi}$ is a weight matrix able to accord physical dimensions. The minimum of $l(\varphi_d)$ can be searched by adopting a trust-region strategy [17], [18]. To this aim, we consider a linear approximation of the equilibrium residual as

$$r_L(\delta\varphi_d) \simeq r_e(\hat{\varphi}_d) + \left.\frac{\partial r_e}{\partial\varphi_d}\right|_{\hat{\varphi}} \delta\varphi_d, \tag{37}$$

and search for a solution by minimizing the quadratic model constructed locally

$$\min_{\delta\varphi_d} = l_Q(\delta\varphi_d) = \frac{1}{2}r_L(\delta\varphi_d)^T W_e r_L(\delta\varphi_d). \tag{38}$$

Observing that, by definition (32), it holds that $\Phi_d^\star := \left.\frac{\partial r_e}{\partial\varphi_d}\right|_{\hat{\varphi}}$, taking into account (37), the function to be minimized can be expressed as

$$l_Q(\varphi_d) = \frac{1}{2}\left[r_e(\hat{\varphi}_d)^T + \delta\varphi_d^T\Phi_d^{\star T}\right]W_e\left[r_e(\hat{\varphi}_d) + \Phi_d^\star\delta\varphi_d.\right] \tag{39}$$

Direct inspection of (39) reveals that the gradient and the Hessian matrix of the quadratic model are easily built from the FGM respectively as

$$\nabla l_Q = \Phi_d^{\star T}W_e r_e(\hat{\varphi}_d), \tag{40}$$

$$H_{l_Q} = \Phi_d^{\star T}W_e\Phi_d^\star. \tag{41}$$

The minimum of the quadratic model (aka Gauss-Newton step) is directly available. However, the chosen trust-region approach imposes to constrain the solution step within a reduced region, where the quadratic model used is descriptive of the behavior of the nonlinear function we are interested in minimizing. With the new value of the dependent variable vector, the residual r_e is evaluated again and the procedure is iterated until predefined convergence criteria are met.

The same idea can be used also to set up an iterative method to regulate the grasp compliance. Instrumental to this

Algorithm 1 Compliance Regulation

Input: $\{\varphi(0),\ C_{\text{des}},\ \epsilon_c,\ \epsilon_{\text{eq}}\}$
$j = 0$;
while $l_c > \epsilon_c$ **do**
  $\varphi(j) \rightarrow \{\varphi_d(j), \varphi_i(j)\}$;
  $k = 0$;
  while $l(\varphi_d(k)) > \epsilon_{\text{eq}}$ **do**
    $l_Q(\delta\varphi_d(k))$ evaluated by eq. (39)
    $\nabla l_Q(\varphi_d(k))$ evaluated by eq. (40)
    $H_{l_Q}(\delta\varphi_d(k))$ evaluated by eq. (41)
    compute $\varphi_d(k+1)$ with a Trust-Region Method;
  end while
  $\Phi_i(\varphi(j)) = [\Phi_d^\star(\varphi(j)) \mid \Phi_i^\star(\varphi(j))]$;
  $c_g(\varphi(j)) \Leftarrow \Phi_i(\varphi(j))$;
  $l_c = r_c^T W_c r_c$
  compute $\varphi(j+1)$ with a Trust-Region Method;
  $j++$;
end while
Output: $\varphi(j),\ C_g$

is a measure of the distances between two matrices. Many choices are possible, but in this context we use the Frobenius norm, according to [19]. Indicating with the lower case the vectorial form of a matrix, such that $c_\bullet = \text{vec}(C_\bullet) \in \mathbb{R}^{36}$, defining the vector $r_c = c_{\text{des}} - c_g(\bar{\varphi})$, we can consider the non linear function to minimize

$$l_c = \frac{1}{2} r_c^T W_c r_c, \tag{42}$$

where the matrix $W_c \in \mathbb{R}^{36\times 36}$ has the same function of the W_e. A trust-region method can be applied again to find a configuration minimizing the compliance distance function (42).

In algorithm 1, a pseudo-code shows the two nested minimization loops. The external loop changes the hand input variables, in order to achieve the desired grasp compliance. At each step of the external loop, the internal one iteratively updates the dependent variables to find an equilibrium configuration.

VI. Numerical Examples

In Fig. 2 a planar gripper, composed by two RRR fingers, is shown. This configuration is used as the initial one in all subsequent examples. On the first joint, J_1, we place the origin of the inertial frame $\{A\}$. Attached to the center of the object, we place the object frame $\{B\}$, parallel to the inertial one. For each joint we consider a reference variable, connected through a spring to the actual link, as shown for joint J_2. The length of the links and the diameter of the sphere is $L = 50$ mm. The contacts are *hard fingers*, and their linear stiffness is $k_c = 10$ N/mm. The starting value of the (variable) joint stiffness is $k_q = 300$ Nmm/rad: in the examples $200 \leq k_{q_i} \leq 400$. A correlation

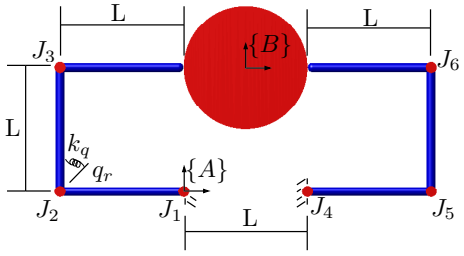

Fig. 2: Sketch of a 2-RRR gripper grasping a ball. This corresponds to the initial configuration of the grasp compliance regulation algorithm in all the examples.

between joint reference angles is introduced via a synergy matrix $S = [s_1^T\ s_2^T\ s_3^T]^T$ where $s_1 = (1, 0, 0, -1, 0, 0)$, $s_2 = (0, 1, 0, 0, -1, 0)$, and $s_3 = (0, 0, 1, 0, 0, -1)$. With this settings, the compliance matrix in the initial configuration results in

$$C_{g_0} = [8.38, 6.31, 0.01, 0, 0.16, 0], \tag{43}$$

where the matrix is flattened according to the rule $[(1,1),(2,2),(3,3),(1,2),(1,3),(2,3)]$.

In Fig. 3, we show the configuration where we computed the *desired* grasp compliance. The object position is identified by $u_{\text{des}} = [0, 100, 0]$, and contact forces are $f_{c_{\text{des}}} = [1, 0, -1, 0]$.

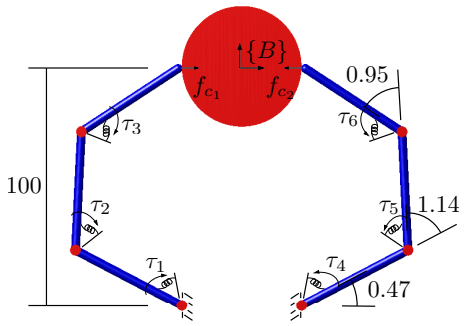

Fig. 3: Configuration corresponding to the target compliance.

The other variables, for the first finger, have the following values

$$\tau = [-100,\ -77.03,\ -27.09],\ \ q = [-0.48,\ 0.43,\ 0.62],\\ \sigma = [-0.76,\ 0.21,\ 0.54], \tag{44}$$

where the joint parameters indicate relative variations with respect to the initial joint configuration. Using $k_q = 350$ for all joints, in this configuration (Fig. 3), the grasp compliance matrix results

$$C_{g_{\text{des}}} = [56.15, 3.64, 0.03, 0, 1.07, 0]. \tag{45}$$

A. Varying Joint Stiffness

Our first test considers the problem of the grasp compliance regulation varying only joint stiffness. Initially, we use as target a grasp compliance matrix obtained in the configuration depicted in Fig. 2, but with $k_q = 350$ for all joints. This ensures that the target compliance is reachable by the system at hand. The target grasp compliance is therefore

$$C_{g_{k_q}} = [7.19, 5.42, 0.01, 0, 0.14, 0]. \tag{46}$$

Employing algorithm 1, the grasp compliance is correctly found, together with the correct joint stiffness values.

Instead, imposing to follow the compliance matrix in (45), the method converges to a minimum corresponding to a joint stiffness vector of the form $k_q = [200,\ 200,\ 400,\ 200,\ 200,\ 400]$, hitting the boundary limits and the obtained compliance results in

$$C_{g_{k_q}} = [12.55, 6.31, 0.01, 0, 0.25, 0]. \tag{47}$$

B. Varying Synergy Variables

Let us consider now the regulation problem using only synergistic variations. Similarly to what seen before, if a compliance target is generated without changing the joint stiffness, the method succeeds in obtaining the target grasp compliance, and the solution perfectly matches the configurations used to define the target.

On the other hand, imposing the matrix (45) as desired, the system can not perfectly achieve the target, arriving to a compliance of the form

$$C_{g_{k_q}} = [56.16, 3.7, 0.03, 0, 1.09, 0]. \tag{48}$$

The system configuration obtained is characterized by the geometry shown in Fig. 4, and, for the first finger, by the following values

$$f_c = [0.75,\ 0,\ 0.75,\ 0],\ \ \tau = [-68.00,\ -60.41,\ -23.36],\\ q = [-0.20,\ 0.01,\ 0.86], \sigma = [-0.42,\ -0.19,\ 0.78]. \tag{49}$$

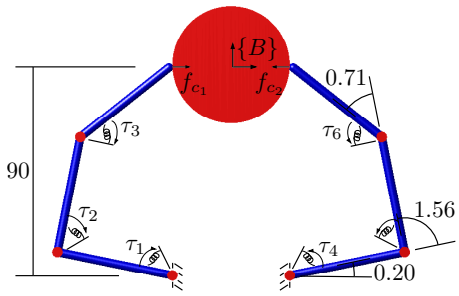

Fig. 4: Configuration found using just the synergistic displacements to obtain the desired compliance.

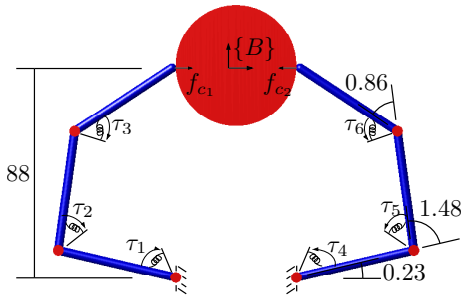

Fig. 5: Configuration found using both the synergistic displacements and joint stiffness control to obtain the desired compliance.

C. Varying Joint Stiffness and Synergy Variables

Finally, we consider the possibility to both vary joint stiffness and synergistic references. In this case, the desired grasp compliance (45) is perfectly achieved, with the configuration depicted in Fig. 5, and with

$$f_c = [0.98,\ 0,\ 0.98,\ 0],\quad \tau = [-87.02,\ -75.82,\ -26.85],$$
$$q = [-0.23,\ 0.09,\ 0.71],\quad \sigma = [-0.56,\ -0.11,\ 0.64]. \tag{50}$$

It is interesting to note that the corresponding configuration found, differs from Fig. 3.

This fact suggests the existence of multiple global solutions, which are not local minima, since the target grasp stiffness has been exaclty achieved (with residual equal to zero up to numerical tolerances). The existence of multiple global solutions allows to specify additional requirements to influence the nature of the solution, for the same reachable grasp stiffness. To this aim, we define a configuration residual, and use it as an additional term in the cost function to be minimized (in the external loop of the algorithm 1). Denoting with φ_m the vector collecting the variables we need to set up, and calling φ_{des} the desired value of this vector, the configuration residual can be written as

$$r_\varphi = \varphi_m - \varphi_{\text{des}}. \tag{51}$$

Taking into account (51), eq. (42) can be substituted with the following

$$l_{c\varphi} = \frac{1}{2} r_c^T W_c r_c + \frac{1}{2} r_\varphi^T W_\varphi r_\varphi. \tag{52}$$

In the case of our example, numerical tests revealed that by introducing the desired object configuration u_{des}, or the desired contact forces $f_{c_{\text{des}}}$, is not enough to recover also the true configuration at which the target compliance was computed. To this aim, a combined use of positions and forces informations is needed, for example setting $\varphi_{\text{des}} = [q_{\text{des}},\ f_{c_{\text{des}}}]$. The investigation of additional goals for biasing the solution configuration towards preferred configurations is the subject of ongoing research.

D. Grasp Compliance Regulation with the DLR/HIT hand II

As an example of a more realistic scenario, we consider the DLR/HIT hand II grasping a ball, as in Fig. 6. For limitation space we do not provide the details of the kinematic model that has been implemented in ADAMS [20]. A synergistic correlation is imposed such that all the reference variable relative to the flex-extension joints have to move of the same quantity. The starting configuration, fig. 6, without contact forces, is characterized by a grasp compliance that, in the translational part, appears as

$$C_{g_0} = [13.26, 11.61, 2.71, 1.28, -4.85, -0.75] \tag{53}$$

Imposing a variation both to the joint stiffness values of $\delta k_q = 100\text{N/mm}$ and to the synergistic reference $\delta\sigma = 0.6$, we arrive at a *loaded* configuration (Fig. 7) characterized by the compliance

$$C_{g_l} = [1.33, 0.05, 0.07, 0.25, 0.29, 0.06]. \tag{54}$$

Using this one as the input for algorithm 1, the solution is perfectly matched in terms of both configuration and joint stiffness values.

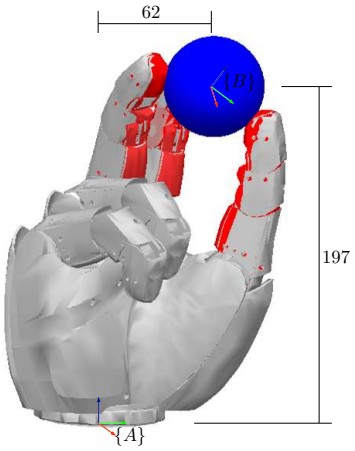

Fig. 6: Starting configuration of the DLR/HIT hand grasping a ball. The red hand represents the reference that attracts the real one. In this case, the contact forces involved are almost null.

From a practical point of view, it is interesting to consider the problem of the physical reachability of the solution proposed. In fact, it is worth observing that the algorithm of compliance regulation gives, as result, an equilibrium solution. However, it does not provide informations about the transition between the starting and the final equilibrium point. To verify the feasibility of the path, the grasping problem was implemented in the multi-body dynamics simulator ADAMS. The resulting mismatch is negligible, especially considering differences in the contact models used. In fact, ADAMS can also consider the contact surface shapes, and the rolling contact, and this can lead to small differences of the final configuration. However, the behavior of the system basically confirm that our results are a good approximation of the steady-state solution of the dynamic simulation.

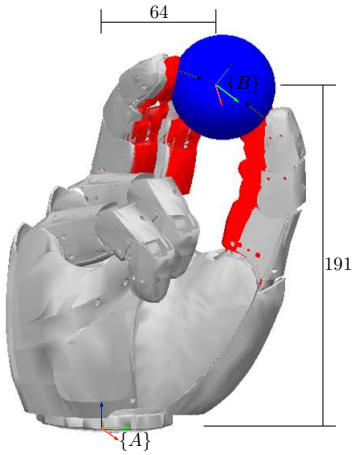

Fig. 7: The present configuration is obtained starting from the tangent one (Fig. 6) and increasing both synergistic references and joint stiffness values. The mismatch between the reference hand and the actual one reflects the force increment.

VII. Conclusion

A general framework to numerically compute and track a predefined grasp compliance is presented. The approach is general enough to consider synergistic underactuated hands, with arbitrary kinematics, endowed with variable stiffness actuators. The method is based on the analytical description of the equilibrium manifold, and of its tangent space at an equilibrium point. While the first one is necessary to guarantee the feasibility of the hand/object configurations, the second one is key for the computation of the grasp compliance matrix. These quantities are the building blocks of an algorithm able to find a new system configuration, where the grasp compliance is automatically steered to a predefined one.

Despite the fact that quasi-static techniques are used, the exploration is not limited to lie to the tangent space and/or to a local neighborhood of the initial equilibrium. This allows to find also solutions far from the initial point, but also to ensure that a path on the equilibrium manifold exists connecting the initial configuration to the desired one. A first numerical test, with a planar 2-RRR hand, posed the problem of achieving a desired grasp (i) changing only the joint compliance values, (ii) changing only the synergistic configuration, (iii) changing both joint stiffness and synergistic configuration. Results show that, when the target compliance is reachable, the methods steers the system towards a solution, where the compliance errors is practically zero. The possibly to have more solutions, in terms of system configurations, for the same target grasp stiffness, suggests the chance to introduce additional specifications to bias the hand/object configurations and/or forces/torques towards preferred behaviors. The presence of multiple global minima (same compliance matrices but different system configurations) requires additional investigations, and will be a subject of future research.

Finally, a dynamic simulation in ADAMS where the DLR/HIT hand II is commanded with the solution found, confirming that the simplifications introduced by the iterative quasi-static approach do not constitute a limiting factor of the method.

References

[1] S. R. C. Ltd., "Shadow hand." Retrieved from Shadowhand: http://shadowhand.com, 2009.

[2] C. S. Lovchik, I. J. N. Gov, and M. A. Diftler, "The robonaut hand: A dexterous robot hand for space," in *in Proc. ICRA*, 1999.

[3] J. Butterfass, M. Grebenstein, H. Liu, and G. Hirzinger, "DLR-hand II: next generation of a dextrous robot hand," in *Robotics and Automation, 2001. Proceedings 2001 ICRA. IEEE International Conference on*, vol. 1, pp. 109–114, 2001.

[4] L. Birglen, T. Laliberté, and C. Gosselin, *Underactuated robotic hands*, vol. 40 of *Springer Tracts in Advanced Robotics*. Springer Verlag, 2008.

[5] A. Bicchi, "Hands for dextrous manipulation and powerful grasping: a difficult road towards simplicity," pp. 2–15, 1996.

[6] C. Y. Brown and H. H. Asada, "Inter-Finger Coordination and Postural Synergies in Robot Hands via Mechanical Implementation of Principal Components Analysis," in *2007 IEEE/RSJ International Conference on Intelligent Robots and System*, pp. 2877–2882, 2007.

[7] M. Ciocarlie, C. Goldfeder, and P. Allen, "Dexterous grasping via eigengrasps: A low-dimensional approach to a high-complexity problem," in *Proceedings of the Robotics: Science & Systems 2007 Workshop-Sensing and Adapting to the Real World, Electronically published*, Citeseer, 2007.

[8] M. Gabiccini, A. Bicchi, D. Prattichizzo, and M. Malvezzi, "On the role of hand synergies in the optimal choice of grasping forces," *Autonomous Robots [special issue on RSS2010]*, vol. 31, no. 2 - 3, pp. 235 – 252, 2011.

[9] M. G. Catalano, G. Grioli, A. Serio, E. Farnioli, C. Piazza, and A. Bicchi, "Adaptive synergies for a humanoid robot hand," in *IEEE-RAS International Conference on Humanoid Robots*, (Osaka, Japan), 2012.

[10] A. D. Luca, "Collision detection and safe reaction with the dlr-iii lightweight manipulator arm," in *IEEE/RSJ International Conference on Intelligent Robots and Systems*, pp. 1623–1630, 2006.

[11] M. Laffranchi, N. Tsagarakis, and D. Caldwell, "Compact arm: a compliant manipulator with intrinsic variable physical damping," in *Proceedings of Robotics: Science and Systems*, (Sydney, Australia), July 2012.

[12] M. Catalano, G. Grioli, M. Garabini, F. Bonomo, M. Mancini, N. Tsagarakis, and A. Bicchi, "Vsa - cubebot. a modular variable stiffness platform for multi degrees of freedom systems," *International Conference on Robotics and Automation*, 2011.

[13] R. Murray, Z. Li, and S. Sastry, *A mathematical introduction to robotic manipulation*. CRC Press, 1994.

[14] M. Gabiccini, E. Farnioli, and A. Bicchi, "Grasp and manipulation analysis for synergistic underactuated hands under general loading conditions," in *International Conference of Robotics and Automation - ICRA 2012*, (Saint Paul, MN, USA), pp. 2836 – 2842, May 14 - 18 2012.

[15] M. Santello, M. Flanders, and J. Soechting, "Postural hand synergies for tool use," *The Journal of Neuroscience*, vol. 18, pp. 10105–10115, December 1998.

[16] C. D. Meyer, ed., *Matrix analysis and applied linear algebra*. Philadelphia, PA, USA: Society for Industrial and Applied Mathematics, 2000.

[17] J. Nocedal and S. J. Wright, *Numerical Optimization*. Springer Series in Operations Research and Financial Engineering, New York, NY, USA: Springer, 2006.

[18] A. R. Conn, N. I. M. Gould, and P. L. Toint, *Trust-region methods*. Philadelphia: SIAM, 2000.

[19] F. Petit and A. Albu-Schffer, "Cartesian impedance control for a variable stiffness robot arm.," in *IROS*, pp. 4180–4186, IEEE.

[20] MSC Software, "Adams: Getting started using adams/view: Version 12," 2002.